# DISTORTIONAL BUCKLING OF STAINLESS STEEL SECTION

Nasim Ahmed*

Athar Hussain**

Sameer Ahmed***

## ABSTRACT

This section of research describes the experimental and numerical investigation of cold-formed, thin-walledstainless steel sections subject to distortional buckling under compression. Austenitic 304,ferritic 430 stainless steel and ferritic-like 3Cr12 chromium weldable steel sheets were brakepressedinto simple-lipped channels and lipped channels with intermediate stiffeners. A full setof coupon tests reveal material nonlinearity with low proportionality stress and low n-parameter,anisotropy and yield strength enhancements up to 2.33 times due to cold-forming. experimental tests and more than 570 finite element tests covering a distortional bucklingslenderness range $0.47 \leq \lambda d \leq 3.64$ and corner to thickness ratios of 1 and 2.5 reveal materialnonlinearity and enhanced corner properties have the most influence on the strength andbehaviour of stainless steel sections and that material anisotropy can be ignored. Enhancedcorner properties may become significant for stocky sections, where $\lambda d < 1$, with a corner area ofat least 10%. Current effective width approach and direct strength methods to design fordistortional buckling of stainless steel and cold-formed carbon steel available. Modified resistance factors arerecommended for the effective width approach of current design codes to meet limit statesdesign criteria. Direct strength design curves are developed for austenitic and ferriticstainlesssteel alloys for inclusion for stainless steel structures.

This section of research also describes the experimental and theoretical investigation of twocommercially available wide-flange, ferritic 445 stainless steel roof sections under purebending. A total of nine tests exhibited distortional buckling behaviour withthe interaction of flange curling. The effects of flange curling and material nonlinearity wereevident as shown by the considerable loss of stiffness in the test results before reaching theultimate load. The theoretical evaluation of flange-curling deformations shows that a truerepresentation of the wide-flange support condition provided by the web is essential to obtainreasonable agreement with experimental tests. The iterative theoretical flange curling

modelwhich represents the changing geometric and loading conditions shows that an average of 6%-17% reduction in yield moment due to reduced section modulus can occur and this is otherwiseignored by the simplified flange curling models. Stresses in the wide-flange can varyconsiderably, with nonlinearity increasing with increasing moment. The most drastic nonlinearbehaviour was exhibited by the more slender section, and, at maximum moment, the centrewideflange stress was only 9% that at web/flange junction. Modified geometries due to flangecurling can cause an increase of critical buckling stress ranging from 1.10 to 3.41 times thatbased on original geometries. Flange curling can produce a net increase of 10.6% for thedistortional buckling design capacity but a net decrease of 12.2% for local buckling capacity.Given the current data, it would be prudent to ignore the effects of flange curling for distortionalbuckling but it would be necessary to consider them for local buckling. The proposed DSMdesign curve developed in this study for distortional buckling of ferritic stainless steel sectionsand the Winter curve for local buckling are generally conservative and suitable given thepresent data.

*Faculty of Technology, CMJ Univ., Shillong, Meghalaya

**Assistant Professor, Deptt. of Civil Engg. GautamBudhUniversity, Gr.Noida

***Assistant Professor Departt. of Civil Engg., Mahamaya Technicial Uni., Noida

## INTRODUCTION

This section of research investigates the distortional buckling of stainless steel sections under compression and bending. This work was inspired by the fact that current design practices for the distortional buckling of stainless steel sections have been uncritically based on those available for cold- formed carbon steel. Cold-formed stainless steel exhibits a nonlinear stress-strain behaviour and has a markedly lower proportionality stress and significant loss of material stiffness beyond this stress. Other material characteristics exhibited by stainless steel include different properties in tension and compression, anisotropy, and significant work hardening capability. Furthermore, each of these characteristics depends on the alloy and the history of cold-working and/or annealing. The influences of these material characteristics on the distortional buckling mode have not been substantiated in the carbon steel-based design guidelines. As such, it has been unclear whether or not the design guidelines are safe for stainless steel. Furthermore, a review of the most currently available literature reveals that there is a lack of data pertaining to the bending of wide-flange stainless steel roof sections, and consequently a lack of design guidance. The behaviour of wide flange sections in bending is further complicated by flange curling, where the wide flange tends to move towards the neutral axis. The flange curling phenomenon is poorly understood and the current literature pertaining to cold-formed carbon steel wide flange sections is lacking. Moreover, to the best of the author's knowledge, the flange curling phenomenon has not been considered for stainless steel sections.

The investigations involve austenitic 304, chromium weldable3Cr12 steel alloy (with properties similar to those of ferritic alloys), and ferritic 430 alloy. The experimental data were used to calibrate finite element models used in numerical studies. All test data were used to evaluate current design procedures available for stainless steel. However, since design codes usually evolve along with cold-formed carbon steel codes, these were examined also. Finally, design recommendations are made for the design of stainless steel sections failing in the distortional buckling mode.

Two commercially available stainless steel roof sections are considered. Distortional/local buckling and flange curling are considered in the experimental tests and analysis. A theoretical analysis of flange curling deformations of cold-formed stainless steel roof

sections and how they affect the stress distributions are examined in detail. The effects of the changing cross-sectional geometry and associated stress redistribution on the strength of the section is also examined. Altered elastic critical buckling stresses due to flange curling are considered in the design recommendations.

The main objectives of this section of study are to develop a greater understanding of the distortional buckling of thin-walled stainless steel sections by considering the material characteristics of stainless steel. Understanding the flange curling phenomenon and how it affects the buckling behaviour is another major objective of this study. The assessment of current design practices and the development of practical design recommendations (with focus on the Direct Strength Method) are the ultimate goals of this work.

## REVIEW OF LITERATURE

Use of stainless steel in construction has been limited due to the high initial cost except in special cases where stainless steel is preferred in a corrosive environment, in the food industry and hospitals where easy cleaning is essential. Not only is stainless steel rust resistant but it also has a higher fire rating than non-treated carbon steel because it maintains stiffness and strength for a longer period of time at higher temperatures. Stainless steel is often preferred over carbon steel by architects who wish to expose the structural elements of an edifice. Although the initial cost of stainless steel is greater than carbon steel, when one considers a life cycle cost analysis, a stainless steel structure could provide the more economical choice.

The most common alloys of stainless steel used in construction fall under three main groups – austenitic, ferritic and duplex. Each group is identified by their microstructure; austenitic alloys have a face-centred atomic structure whereas ferritic stainless steels have a body centred atomic structure and duplex alloys are a cross between austenitic and ferritic alloys and thus have a mixed crystal structure. Austenitic and duplex stainless steel grades as well as the chromium weldable steel 3Cr12 are most popular in construction because of their strength, weldability and corrosion resistance whereas ferritic alloys have poor weldability and are typically available in thin gauges and thus are used mainly for decorative purposes (AS/NZS2001). The specific alloys considered in this study are the austenitic 304, ferritic 430, ferritic445 and ferritic-like chromium weldable steel 3Cr12. The material characteristics vary for each alloy but generally all exhibit a low proportionality stress with

significant loss of stiffness beyond this stress (i.e. rounded stress strain curve without a distinct yield point) and strength enhancement capability due to cold-working. Furthermore, stainless steel exhibits anisotropy and has different strengths in the longitudinal and transverse directions (with respect to rolling) and the material properties are different in compression and tension.

The research into stainless steel structures is, compared to carbon-steel, recent and the earliest design specification for cold-formed stainless steel structural members was produced by the American Iron and Steel Institute (AISI 1968). Since then, the code has undergone revisions, either to account for research developments in the stainless steel field or to conform to the changes in the cold-formed carbon steel codes. The Chromium Steels Research Group at the Rand Afrikaans University, South Africa and University of Missouri-Rolla, USA undertook a major research effort on stainless steel structures and contributed to the development of the North American-based American Society of Civil Engineers Standard (ASCE 2002). The latest Australian and New Zealand design standard for cold-formed stainless steel was published in2001 (AS/NZS:4673 2001) and the latest pre-standard design specification proposed for use in Europe is the Eurocode 3: Part 1-4 (preEN-1993-Part.1-4 2004), henceforth referred to as the EC3Part1-4. The pre-standard EC3 Part 1-4 (2004) has been adopted from the Euro-Inox "Design Manual for Structural Stainless Steel" (2002) which was developed as a result of a major research effort supported by the European Coal and Steel Community (ECSC), the Nickel Development Institute and stainless steel producers in the UK, Sweden, Finland, France, Germany and Italy (Burgan et al. 2000).

The ASCE (2002), AS/NZS:4673 (2001) and EC3Part1-4 design guidelines for distortional buckling will be assessed in this study. Apart from the EC3Part1-4 strength curve for local plate buckling, which is more conservative than that proposed for cold-formed carbon steel, the guidelines are identical to those found in the cold-formed carbon steel based codes. There has been very little research in the area of distortional buckling of stainless steel sections. Recognition is given to Buitendag and van den Berg (1994), and van den Berg (2000) who have conducted tests on partially stiffened sections. In their work, they have proposed the use of a plasticity reduction factor to take into account the loss of stiffness in the design procedures. However, this leads to iterative calculations and may not be suitable

for design engineers. Their proposal is further examined in the following section of the literature review which focuses on the distortional buckling mode.

Some of the major developments in recent stainless steel construction research regarding member behaviour are recognized and briefly listed here for the reader's reference. Developments with respect to material modelling which focus on the description of the stress- strain curve (Rasmussen 2003), (Rasmussen et al. 2003); stainless steel plasticity and constitutive modelling incorporating the influence of anisotropy (Olsson 1998), (Johansson and Olsson 2000), (Gozzi 2004); evaluation and prediction of enhanced corner properties due to cold-working (van den Berg and van der Merwe 1992), (Ashraf et al. 2005), column behaviour (Gardner and Nethercot2004a), (Gardner and Nethercot2004b), (Rasmussen and Rondal 1997), (Rasmussen and Rondal 2000), (Rasmussen 2000), (Bredenkamp and van den Berg 1995), plate behaviour (Bezkorovainy et al. 2003), (Rasmussen et al. 2003); deflections (Mirambell and Real 2000), residual stresses (Bredenkamp and van den Berg 1995), beams and/or girders (Rasmussen and Hancock 1992), (Mirambell and Real 2000), (Gardner and Nethercot2004b), (Kouhi et al. 2000), (Lagerqvist and Olsson 2001), generalized beam theory for stainless steel (Goncalves and Camotim 2004), behaviour of partially stiffened opened sections (Buitendag and van den Berg 1994). The most relevant of these references to the research topic of distortional buckling behaviour of stainless steel sections are discussed in greater detail in the following sections and throughout the study.

## MATERIALS AND METHODS

Stainless steel is defined as a steel alloy with a minimum of 10.5 weight percent chromium. Although stainless steel does not generally corrode as easily as ordinary steel, different grades are necessary for different environments. For example, several manufacturing groups (including semiconductor and pharmaceutical) have stringent requirements for stainless steel surfaces.

The corrosion-resistant properties of stainless steel are due to the formation of a passive chromium oxide layer. Although this layer forms naturally when the material is exposed to the atmosphere, additional chemical treatments (passivation) can improve the relative amount of chromium at the surface.

The surface chemistry changes due to passivation occur within the outer ~50Å of the surface. In order to measure these changes, surface analytical tools such as x-ray photoelectron spectroscopy (XPS) and Auger electron spectroscopy (AES) are necessary. One of the stainless steel measurements that is made using Auger and XPS is the near-surface chromium/iron (Cr/Fe) ratio.

When stainless steel is analyzed with Auger:

- A survey scan determines the overall elemental composition of the surface from atomic numbers 3-92. This yields the surface Cr/Fe ratio.
- If the analysis is conducted with XPS, the major elements detected (usually carbon, oxygen, silicon, chromium, iron, nickel, and molybdenum) are analyzed in high energy resolution mode to determine their binding energies and then to make some inferences about the compounds present on the surface. The ratio of chromium oxide to chromium metal, and iron oxide to iron metal, is obtained. The distribution of organic states is measured.
- A third step in the analysis includes a depth profile to determine the concentration of the primary elements as a function of depth. This also yields the Cr/Fe ratio as a function of depth.
- A final survey scan is obtained. This is useful for internal calibration.

Distortional buckling is a special kind of buckling mode, which is less well known. Researchers have recently paid more attention to this problem. For stainless steel structures, it is necessary to investigate their behaviour when distortional buckling occurs. In this project, the distortional buckling of cold-formed stainless steel columns under axial compression is investigated. The finite element method is used to analyse and calculate different buckling modes, especially distortional buckling. This is compared to experimental results and other theoretical predictions.

## EXPERIMENTAL OBSERVATIONS

A total of nine bending tests were conducted successfully. A summary of the internal reaction forces at the specimens south and north ends, as obtained in study, are given in Tables 1 to 9 for each test, followed by the moment versus rotation plots in Figures 1 to 9. The data listed in the tables are for every load step/profile reading identified in the load/profile ID column. For example, “L1/P1” in Table 1 indicates end of load step 1 and

profile 1 and the shear, axial and moment reactions and rotations are listed. These points can be related to the plot in Figure 1 which shows the internal moment versus rotation of the south and north ends. In Figure 1 the points where profile readings were taken are highlighted by the labels “P1 to P10” and the deflection plots corresponding to these points are detailed for every LVDT in study. The moment versus rotation plots are given in Figures 1 to 9 and show some of the section geometric properties and the calculated initial modulus of elasticity.

**Table 1 : Internal Reactions MONO 1**

| *MONO1* | South End Internal Reactions | | | | North End Internal Reactions | | | |
|---|---|---|---|---|---|---|---|---|
| | $V_S$ | $N_S$ | $M_S$ | $Rot_S$ | $V_N$ | $N_N$ | $M_N$ | $Rot_N$ |
| Load/Profile ID | N | N | Nm | radians | N | N | Nm | radians |
| L1/P1 | 34 | -451 | -299 | 0.0202 | 20 | -452 | -253 | 0.0194 |
| L2/P2 | 74 | -637 | -470 | 0.0331 | 38 | -641 | -390 | 0.0321 |
| L3/P3 | 50 | -651 | -570 | 0.0402 | 3 | -653 | -472 | 0.0403 |
| L4/P4 | 78 | -788 | -703 | 0.0543 | 0 | -792 | -635 | 0.0532 |
| L5/P5 | 92 | -831 | -790 | 0.0681 | -14 | -836 | -721 | 0.0680 |
| ***Maximum, South End*** | ***47*** | ***-665*** | ***-867*** | ***0.0947*** | ***-64*** | ***-637*** | ***-869*** | ***0.0928*** |
| L6/P6 | 54 | -638 | -858 | 0.0981 | -102 | -500 | -897 | 0.0955 |
| L7/P7 | 6 | -511 | -815 | 0.1114 | -72 | -663 | -889 | 0.1099 |
| ***Maximum, North End*** | ***-7*** | ***-380*** | ***-809*** | ***0.1309*** | ***-101*** | ***-366*** | ***-901*** | ***0.1298*** |
| L8/P8 | -6 | -380 | -810 | 0.1309 | -101 | -366 | -901 | 0.1299 |
| L9/P9 | -33 | -236 | -783 | 0.1530 | -101 | -216 | -897 | 0.1540 |
| L10/P10 | -93 | -31 | -714 | 0.1803 | -98 | 4 | -875 | 0.1939 |

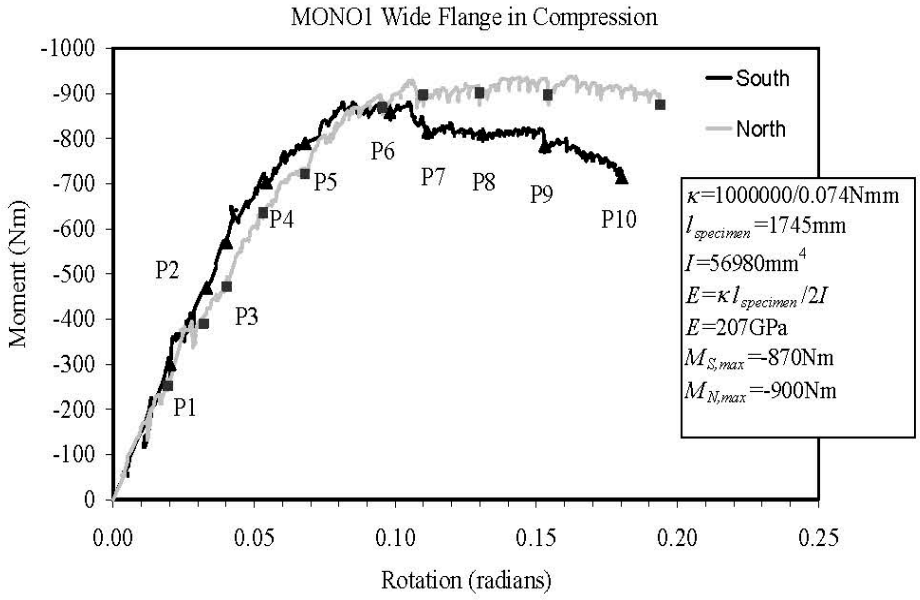


**Figure 1 : Moment versus Rotation MONO 1**

**Table 2 : Internal Reactions MONO 2**

| *MONO2* | South End Internal Reactions | | | | North End Internal Reactions | | | |
|---|---|---|---|---|---|---|---|---|
| | $V_S$ | $N_S$ | $M_S$ | $Rot_S$ | $V_N$ | $N_N$ | $M_N$ | $Rot_N$ |
| Load/Profile ID | N | N | Nm | radians | N | N | Nm | radians |
| L1/P1 | 26 | -222 | -145 | 0.0123 | 20 | -223 | -106 | 0.0131 |
| L2/P2 | 66 | -472 | -416 | 0.0283 | 39 | -475 | -329 | 0.0283 |
| L3/P3 | 63 | -579 | -617 | 0.0471 | 7 | -583 | -559 | 0.0479 |
| L4/P4 | 50 | -587 | -741 | 0.0653 | -27 | -588 | -723 | 0.0649 |
| L5/P5 | 28 | -523 | -811 | 0.0874 | -63 | -520 | -841 | 0.0870 |
| ***Maximum, South End*** | ***36*** | ***-489*** | ***-843*** | ***0.0971*** | ***-59*** | ***-487*** | ***-862*** | ***0.0958*** |
| ***Maximum, North End*** | ***15*** | ***-449*** | ***-821*** | ***0.1018*** | ***-75*** | ***-443*** | ***-872*** | ***0.1000*** |
| L6/P6 | -1 | -387 | -762 | 0.1059 | -82 | -378 | -831 | 0.1057 |
| L7/P7 (not in appendix) | 14 | -293 | -803 | 0.1260 | -59 | -288 | -841 | 0.1258 |
| L8/P8 | 5 | -163 | -799 | 0.1508 | -44 | -157 | -831 | 0.1505 |
| L8/P8 | 9 | 21 | -605 | 0.1765 | 16 | 16 | -584 | 0.1789 |

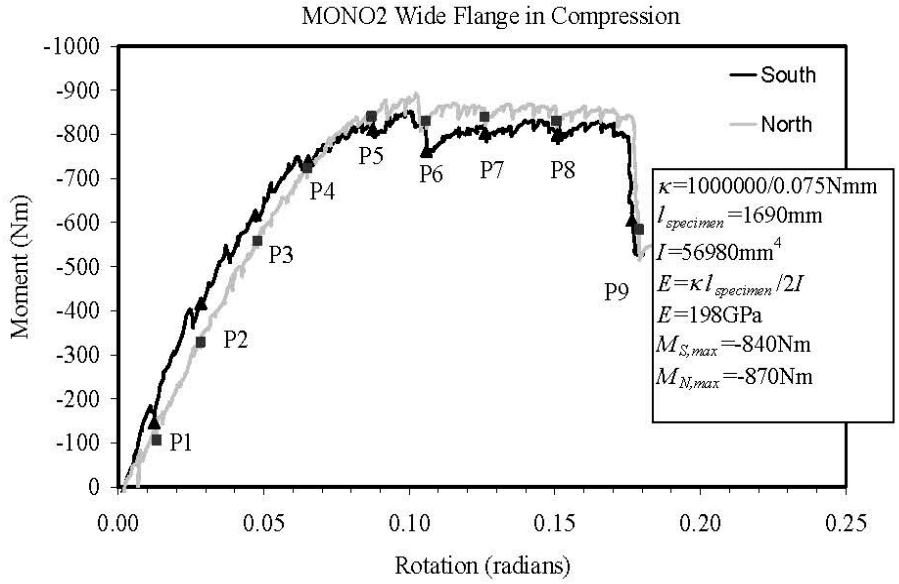


**Figure 2 : Moment versus Rotation MONO 2**

**Table 3 : Internal Reactions MONO 3**

| *MONO3* | South End Internal Reactions | | | | North End Internal Reactions | | | |
|---|---|---|---|---|---|---|---|---|
| | $V_S$ | $N_S$ | $M_S$ | $Rot_S$ | $V_N$ | $N_N$ | $M_N$ | $Rot_N$ |
| Load/Profile ID | N | N | Nm | radians | N | N | Nm | radians |
| L1/P1 | 13 | -249 | -76 | 0.0063 | 8 | -249 | -58 | 0.0070 |
| L2/P2 | 27 | -482 | -341 | 0.0274 | -2 | -482 | -322 | 0.0253 |
| L3/P3 | -12 | -550 | -486 | 0.0418 | -62 | -546 | -548 | 0.0420 |
| L4/P4 | 34 | -619 | -656 | 0.0600 | -45 | -618 | -666 | 0.0590 |
| L5/P5 | 46 | -593 | -792 | 0.0815 | -55 | -592 | -800 | 0.0815 |
| L6/P6 | 66 | -534 | -845 | 0.0958 | -41 | -537 | -824 | 0.0958 |
| ***Maximum, South End L7/P7*** | ***83*** | ***-455*** | ***-870*** | ***0.1105*** | ***-22*** | ***-462*** | ***-820*** | ***0.1087*** |
| L8/P8 | 62 | -378 | -854 | 0.1196 | -33 | -381 | -830 | 0.1201 |
| ***Maximum, North End*** | ***-52*** | ***-262*** | ***-761*** | ***0.1273*** | ***-121*** | ***-238*** | ***-900*** | ***0.1387*** |
| L9/P9 | -31 | -208 | -792 | 0.1365 | -90 | -191 | -887 | 0.1493 |
| L10/P10 | -16 | 29 | -685 | 0.1690 | -5 | 32 | -702 | 0.1871 |

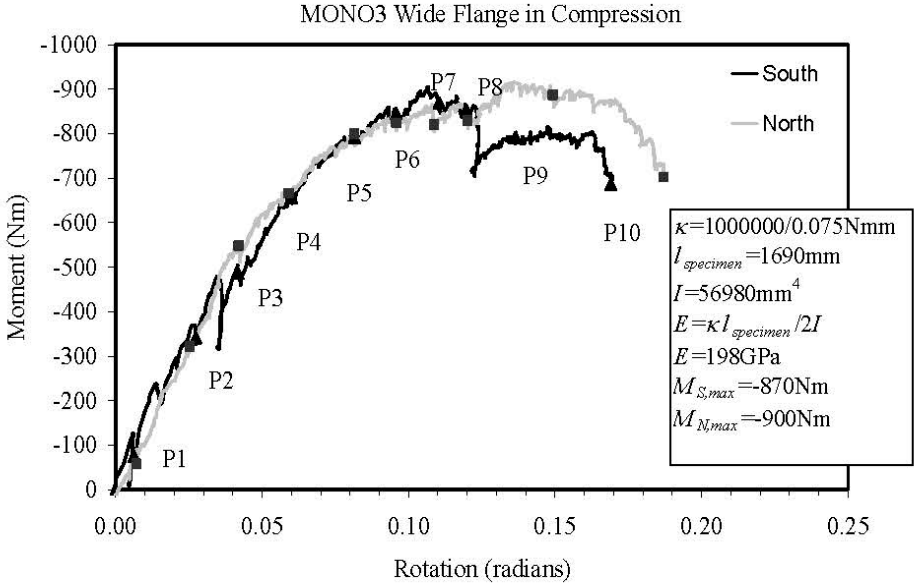


**Figure 3 : Moments Vs. Rotation MONO 3**

**Table 4 : Internal Reactions MONO 7**

| *MONO7* | South End Internal Reactions | | | | North End Internal Reactions | | | |
|---|---|---|---|---|---|---|---|---|
| | $V_S$ | $N_S$ | $M_S$ | $Rot_S$* | $V_N$ | $N_N$ | $M_N$ | $Rot_N$* |
| Load/Profile ID | N | N | Nm | radians | N | N | Nm | radians |
| L1/P1 | 11 | -600 | -414 | 0.0264 | -11 | -600 | -414 | 0.0266 |
| L2/P2 | 131 | -945 | -760 | 0.0481 | 53 | -952 | -686 | 0.0474 |
| L3/P3 | 64 | -862 | -782 | 0.0597 | -33 | -863 | -748 | 0.0579 |
| L4/P4 | N/A | | | | | | | |
| L5/P5 | | | | | | | | |
| L6/P6 | 129 | -523 | -1212 | 0.1276 | 3 | -539 | -1146 | 0.1272 |
| L7/P7 | 72 | -331 | -1175 | 0.1462 | -21 | -338 | -1134 | 0.1449 |
| ***Maximum, South End*** | ***121*** | ***-743*** | ***-1194*** | ***0.1346*** | ***-59*** | ***-750*** | ***-1154*** | ***0.1110*** |
| ***Maximum, North End*** | ***64*** | ***-333*** | ***-1178*** | ***0.1462*** | ***-29*** | ***-338*** | ***-1150*** | ***0.1347*** |
| L8/P8 | 126 | 43 | -871 | 0.1702 | 133 | -2 | -662 | 0.1765 |

* Adjusted for Experimental Error

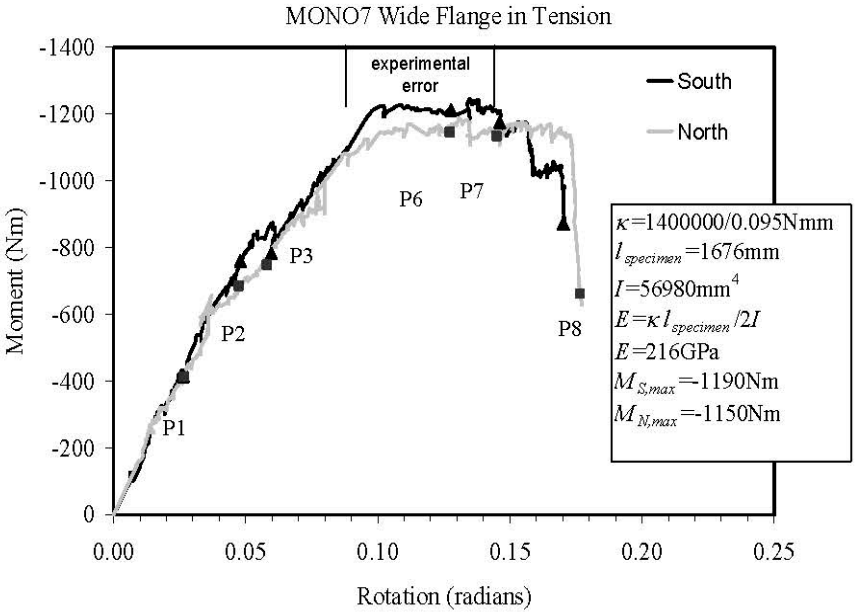


**Figure 4 : Moment Vs. Rotation MONO 7**

**Table 5 : Internal Reactions MONO 8**

| *MONO8* | South End Internal Reactions | | | | North End Internal Reactions | | | |
|---|---|---|---|---|---|---|---|---|
| | $V_S$ | $N_S$ | $M_S$ | $Rot_S$ | $V_N$ | $N_N$ | $M_N$ | $Rot_N$ |
| Load/Profile ID | N | N | Nm | radians | N | N | Nm | radians |
| L1/P1 | 14 | -512 | -424 | 0.0259 | -5 | -512 | -415 | 0.0265 |
| L2/P2 | 49 | -666 | -712 | 0.0460 | -2 | -668 | -674 | 0.0463 |
| L3/P3 | 43 | -697 | -928 | 0.0653 | -37 | -698 | -923 | 0.0657 |
| L4/P4 | 103 | -640 | -1035 | 0.0812 | 10 | -649 | -945 | 0.0794 |
| L5/P5 | 24 | -467 | -1053 | 0.1020 | -63 | -464 | -1085 | 0.1016 |
| ***Maximum, South End*** | ***55*** | ***-347*** | ***-1130*** | ***0.1207*** | ***-23*** | ***-351*** | ***-1106*** | ***0.1183*** |
| ***Maximum, North End*** | ***29*** | ***-337*** | ***-1114*** | ***0.1211*** | ***-47*** | ***-335*** | ***-1128*** | ***0.1195*** |
| L6/P6 | 23 | -292 | -1101 | 0.1248 | -45 | -289 | -1118 | 0.1245 |
| L7/P7 | 9 | -94 | -1081 | 0.1494 | -18 | -93 | -1088 | 0.1461 |
| L8/P8 | -74 | 95 | -999 | 0.1695 | -39 | 113 | -1088 | 0.1747 |
| L9/P9 | 35 | 220 | -762 | 0.1838 | 110 | 194 | -650 | 0.1894 |

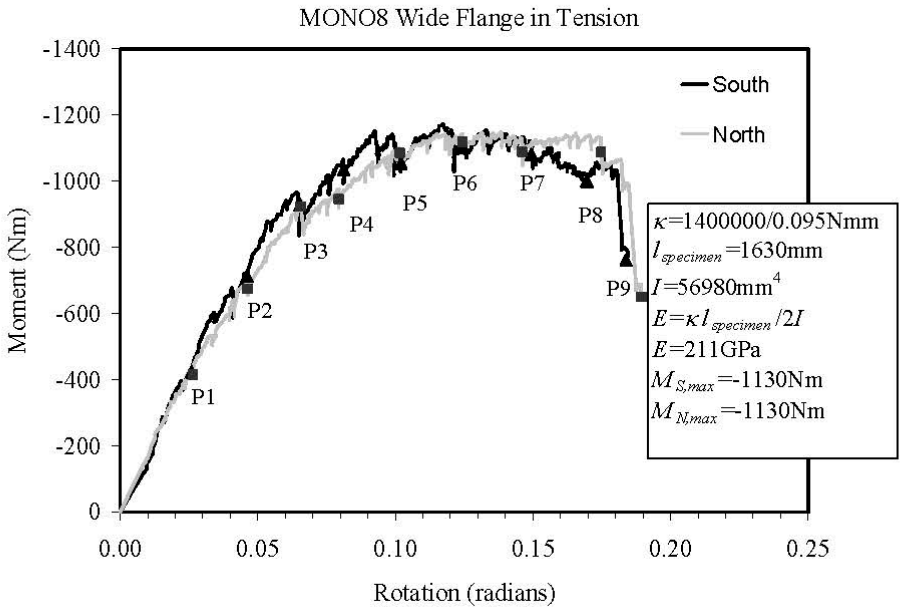


**Figure 5 : Moment Vs. Rotation MONO 8**

**Table 6 : Internal Reactions MEGA1**

| *MEGA1* | South End Internal Reactions | | | | North End Internal Reactions | | | |
|---|---|---|---|---|---|---|---|---|
| | $V_S$ | $N_S$ | $M_S$ | $Rot_S$ | $V_N$ | $N_N$ | $M_N$ | $Rot_N$ |
| Load/Profile ID | N | N | Nm | radians | N | N | Nm | radians |
| L1/P1 | 31 | -661 | -358 | 0.0298 | 5 | -662 | -328 | 0.0296 |
| L2/P2 | 26 | -701 | -454 | 0.0466 | -25 | -701 | -453 | 0.0467 |
| L3/P3 | 34 | -710 | -515 | 0.0589 | -35 | -710 | -517 | 0.0586 |
| L4/P4 | 37 | -688 | -561 | 0.0720 | -48 | -687 | -570 | 0.0724 |
| L5/P5 | 27 | -551 | -520 | 0.0903 | -62 | -549 | -550 | 0.0900 |
| L6/P6 | 48 | -544 | -625 | 0.1091 | -60 | -543 | -635 | 0.1088 |
| L7/P7 | 39 | -497 | -626 | 0.1168 | -67 | -494 | -649 | 0.1171 |
| L8/P8 | 42 | -385 | -649 | 0.1397 | -58 | -383 | -662 | 0.1388 |
| L9/P9 | 25 | -265 | -662 | 0.1624 | -55 | -261 | -687 | 0.1615 |
| ***Maximum, South and North Ends*** | ***24*** | ***-257*** | ***-667*** | ***0.1639*** | ***-55*** | ***-252*** | ***-692*** | ***0.1642*** |
| L10/P10 | -6 | -85 | -604 | 0.1896 | -37 | -78 | -638 | 0.1961 |

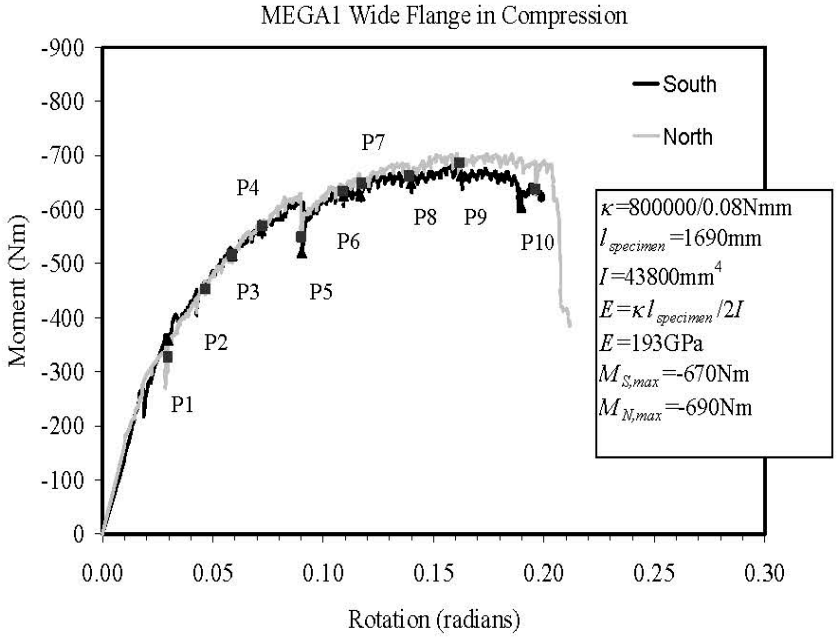


**Figure 6 : Moment Vs. Rotation MEGA1**

**Table 7 : Internal Reactions MEGA2**

| *MEGA2* | South End Internal Reactions | | | | North End Internal Reactions | | | |
|---|---|---|---|---|---|---|---|---|
| | $V_S$ | $N_S$ | $M_S$ | $Rot_S$ | $V_N$ | $N_N$ | $M_N$ | $Rot_N$ |
| Load/Profile ID | N | N | Nm | radians | N | N | Nm | radians |
| L1/P1 | 30 | -563 | -232 | 0.0212 | 12 | -563 | -197 | 0.0212 |
| L2/P2 | 80 | -781 | -437 | 0.0424 | 22 | -785 | -352 | 0.0420 |
| L3/P3 | 76 | -766 | -475 | 0.0535 | 2 | -770 | -409 | 0.0537 |
| L4/P4 | 90 | -789 | -578 | 0.0717 | -16 | -794 | -516 | 0.0719 |
| L5/P5 | 115 | -742 | -660 | 0.0943 | -19 | -751 | -580 | 0.0942 |
| L6/P6 | 107 | -611 | -697 | 0.1186 | -34 | -620 | -636 | 0.1192 |
| L7/P7 | 113 | -537 | -729 | 0.1335 | -27 | -548 | -657 | 0.1333 |
| ***Maximum, South End*** | ***122*** | ***-503*** | ***-745*** | ***0.1415*** | ***-17*** | ***-518*** | ***-660*** | ***0.1389*** |
| ***Maximum, North End*** | ***75*** | ***-356*** | ***-723*** | ***0.1598*** | ***-38*** | ***-362*** | ***-691*** | ***0.1625*** |
| L8/P8 | 75 | -354 | -717 | 0.1597 | -37 | -360 | -685 | 0.1625 |
| L9/P9 | 40 | -177 | -708 | 0.1864 | -26 | -180 | -696 | 0.1909 |

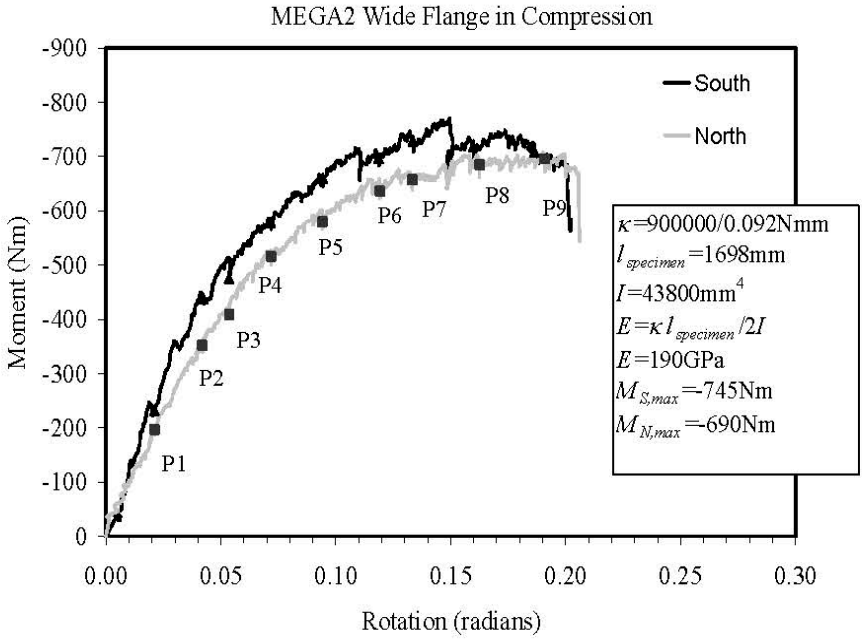


**Table 7 :Moment Vs. Rotation MEGA2**

**Table 8 : Internal Reactions MEGA3**

| *MEGA3* | South End Internal Reactions | | | | North End Internal Reactions | | | |
|---|---|---|---|---|---|---|---|---|
| | $V_S$ | $N_S$ | $M_S$ | $Rot_S$ | $V_N$ | $N_N$ | $M_N$ | $Rot_N$ |
| Load/Profile ID | N | N | Nm | radians | N | N | Nm | radians |
| L1/P1 | 27 | -448 | -282 | 0.0218 | 8 | -449 | -252 | 0.0222 |
| L2/P2 | 38 | -527 | -435 | 0.0411 | -5 | -529 | -408 | 0.0404 |
| L3/P3 | 59 | -522 | -573 | 0.0651 | -13 | -525 | -531 | 0.0712 |
| L4/P4 | 120 | -535 | -685 | 0.0805 | 32 | -547 | -560 | 0.0820 |
| L5/P5 | 104 | -471 | -716 | 0.0935 | 14 | -482 | -619 | 0.0950 |
| L6/P6 | 109 | -429 | -738 | 0.1034 | 19 | -442 | -633 | 0.1031 |
| L7/P7 | 124 | -395 | -746 | 0.1098 | 35 | -412 | -616 | 0.1096 |
| L8/P8 | 109 | -313 | -764 | 0.1251 | 29 | -330 | -651 | 0.1234 |
| ***Maximum, South End*** | ***102*** | ***-307*** | ***-777*** | ***0.1262*** | ***23*** | ***-323*** | ***-675*** | ***0.1250*** |
| L9/P9 | -6 | -173 | -677 | 0.1440 | -55 | -164 | -727 | 0.1449 |
| ***Maximum, North End*** | ***-39*** | ***-99*** | ***-667*** | ***0.1593*** | ***-68*** | ***-82*** | ***-753*** | ***0.1595*** |
| L10/P10 | -3 | -42 | -572 | 0.1658 | -16 | -39 | -587 | 0.1676 |

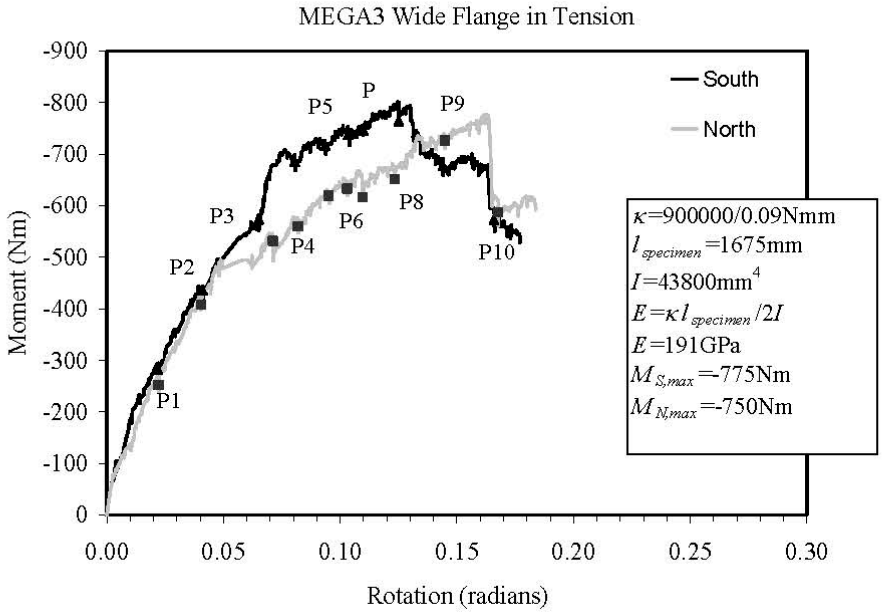


**Figure 8 :Moment Vs. Rotation MEGA3**

**Table 9 : Internal Reactions MEGA4**

| *MEGA4* | South End Internal Reactions | | | | North End Internal Reactions | | | |
|---|---|---|---|---|---|---|---|---|
| | $V_S$ | $N_S$ | $M_S$ | $Rot_S$ | $V_N$ | $N_N$ | $M_N$ | $Rot_N$ |
| Load/Profile ID | N | N | Nm | radians | N | N | Nm | radians |
| L1/P1 | 63 | -594 | -306 | 0.0238 | 43 | -596 | -217 | 0.0241 |
| L2/P2 | 90 | -735 | -452 | 0.0350 | 49 | -739 | -335 | 0.0353 |
| L3/P3 | 71 | -698 | -464 | 0.0431 | 18 | -702 | -387 | 0.0457 |
| L4/P4 | 104 | -804 | -585 | 0.0511 | 31 | -810 | -470 | 0.0531 |
| L5/P5 | 122 | -819 | -638 | 0.0591 | 35 | -828 | -505 | 0.0610 |
| L6/P6 | 146 | -800 | -726 | 0.0763 | 33 | -813 | -577 | 0.0776 |
| L7/P7 | 161 | -725 | -787 | 0.0957 | 30 | -742 | -629 | 0.0960 |
| ***Maximum, South End*** | ***173*** | ***-657*** | ***-834*** | ***0.1107*** | ***34*** | ***-678*** | ***-663*** | ***0.1104*** |
| L8/P8 | 125 | -580 | -758 | 0.1140 | 1 | -593 | -655 | 0.1119 |
| L9/P9 | -103 | -262 | -550 | 0.1489 | -172 | -223 | -776 | 0.1483 |
| ***Maximum, North End*** | ***-144*** | ***-177*** | ***-545*** | ***0.1706*** | ***-193*** | ***-121*** | ***-820*** | ***0.1704*** |
| L10/P10 | -4 | -82 | -497 | 0.1822 | -33 | -75 | -526 | 0.1903 |

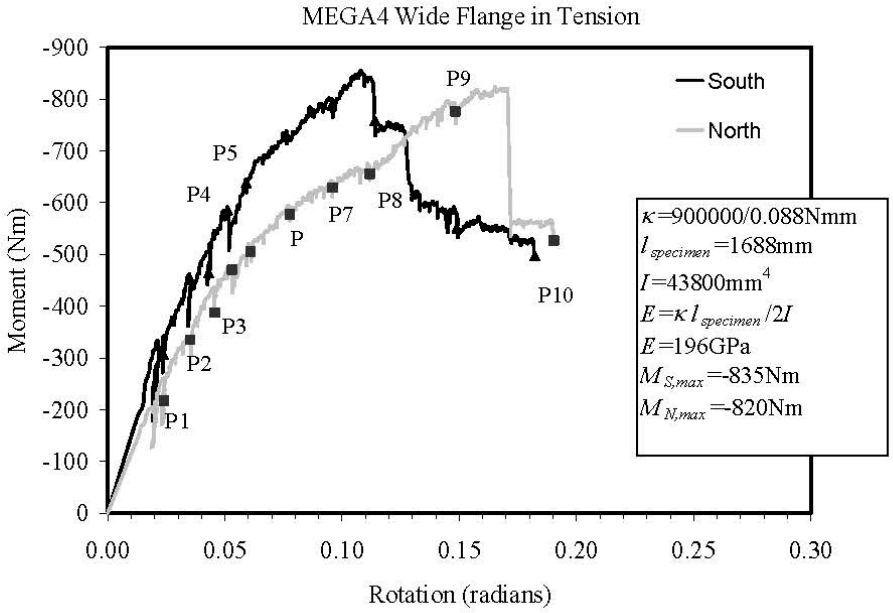


**Figure 9 :Moment Vs. Rotation MEGA4**

A few observations can be made from Tables 1-9 and Figures 1-9. As shown in Tables 1-9, for every test there is an initial axial tension which generally begins to increase as the applied load increases. However, as the south load cell approaches a vertical position the axial force begins to drop and if it goes beyond vertical the applied load becomes compressive. Also, generally there is an increase in shear until it drops, once the maximum moment is reached. In any case, the internal axial and shear forces are small and can be neglected. Furthermore, as shown in Tables 1 to 9, the calculated south and north end

moments are in fair agreement and the mid-span moment can be estimated as the average of the two. The calculation of the initial modulus of elasticity for each test is shown in Figures 1 to 9 and they are comparable with the modulus of elasticity determined from coupon tests. As expected, all tests showed considerable roundedness in the moment versus rotation graphs and this can be attributed to the characteristic behaviour of stainless steel nonlinearity, to the flange curling phenomenon, as described by Bernard et al. (1993a), and to the development of distortional and/or local buckling deformations. More specifically, the roundedness of the moment versus rotation graph is apparently greater for sections tested with the wide flange in compression, which include MONO1, MONO2, MONO3, MEGA1 and MEGA2 than for those sections tested with the wide flange in tension. The MONO test series which had a second moment of area (based on average gross cross-sectional properties), I, 30% larger than the MEGA tests provided a stiffer response and greater ultimate load. All tests reached ultimate load by a spatial plastic collapse mechanism in the main strengthening ribs and the site of the collapse varied for each test but generally occurred in the middle third of the test specimens. The exceptions to this are test specimens MEGA3 and MEGA4 which both had imperfections, introduced from the manufacturing cutting procedures, in the flange of the strengthening ribs at approximately $1/7^{th}$ of the specimen length from the south end. The locations of these local imperfections are the sites where the spatial plastic collapse mechanism initiated for MEGA3 and MEGA4.

## RESULTS AND CONCLUSION

### Distortional buckling of Stainless Steel Compression Members

Current design guidelines to asses the distortional buckling of thin-walled, cold-formed stainless steel lipped channels with or without intermediate stiffeners have been uncritically based on those available for cold-formed carbon steel codes overlooking the material properties characteristic of stainless steel alloys. It is well known that stainless steel has a low proportionality stress, a low “n” parameter, is anisotropic and has the potential for strength enhancements due to cold-working. The purpose of the research study, presented herein, was to examine the influence of stainless steel material characteristics on the distortional buckling behaviour of compression members and to use experimental and finite element results to critically assess design practices. The AS/NZS 4673 (2001), the ASCE (2002) and EuroCode 3 Part 1-4/Part 1-3 codes for coldformed stainless steel use the

Effective Width Approach (EWA) to determine the distortional buckling strength and are essentially identical to the cold-formed carbon steel EWA procedures. More recently, the Direct Strength Method (DSM) has been adopted in the cold-formed carbon steel codes AS/NZS 4600 (1996) and the North American Standard NAS as alternative to the EWA. Anticipating that the efficient DSM would also be adopted in the stainless steel codes, evaluating current DSM curves became an essential part of the design code evaluations..

**Buckling and Flange Curling of Wide-Flange Sections in Bending**

The experimental and analytical investigation of the distortional/local buckling and flange curling of wide-flanged stainless steel roof sections have been presented. The goals of the experimental programme were to develop i) a test rig which allowed essentially pure bending moment to develop in the wide flange sections, ii) capture the flange curling and buckling deformations, and iii) capture the stainless steel nonlinear material behaviour. The flange curling phenomenon has previously been given little attention, as was evident by the limited available literature. Any literature that is available is based on studies of cold-formed carbon steel so, to the best of the author's knowledge, this study presents the first set of results for stainless steel wide flange sections and also the first attempt to analytically model the nonlinear flange curling problem accounting for geometrical changes. The main goals of the analytical investigation were to determine the nonlinear flange curling deformations, changes in geometric properties and stresses in the wide flange section. The effect of stress redistribution on the distortional and local buckling behaviour formed an important part of the analytical study and design evaluations.

Two commercially available ferric 445 stainless steel roof-sections were tested under pure bending conditions. The test rig used for this experimental programme was similar in concept to one used in previous studies conducted by Bernard et al. (1996), but was specifically designed to accommodate the pure bending of stainless steel wide flange roof specimens. Considerable effort was put into the test rig design to capture flange curling and distortional buckling deformations. A total of 9 bending tests, with the wide flange oriented so that it was either in tension or compression, were successfully conducted. Distortional buckling was evident when the wide flange was in compression whereas local buckling of the rib stiffener was predominant when the wide flange was in tension. All sections exhibited nonlinear moment-rotation behaviour at ultimate moment.

## RECOMMENDATION

A significant amount of data has been produced by the efforts of the author. Great care was exercised in the preparation and execution of tests, collection and analysis of data to ensure the soundness of results. There is now a better understanding of the distortional buckling behaviour of stainless steel sections, a significant advancement in the theory of flange curling and ample data available for future use. Continued research on the distortional buckling and the flange curling phenomena would ultimately lead to improved stainless steel design guidelines. Some recommendations for further study are discussed below.

The distortional buckling study presented herein was limited to austenitic and ferritic stainless steel alloys. The exploration of duplex stainless steel sections subject to distortional buckling would also be warranted. Duplex alloys are mixed compositions of austenitic and ferritic alloys and it would be reasonable to predict that the distortional buckling strengths of duplex stainless steel sections would fall between those obtained from austentic and ferritic stainless steel sections. Given the current lack of data, it would be sensible to use the design recommendations which have been developed for austenitic stainless. Future studies may reveal that another set of design recommendations for duplex alloys is needed to prevent over conservatism. Furthermore, this particular study was limited to compression members that fail by the distortional buckling mode. Combined failure modes, such as the distortional and local interaction buckling, would require investigation. Moreover, sections made from hardened stainless steel material would broaden the understanding of the effects of enhanced strength properties on the distortional buckling behaviour. Additionally, it may be a worthwhile exercise to develop an effective width model which theoretically captures the stainless steel material nonlinearity. However, this would lead to a sophisticated set of design procedures that involve iteration and may not be suitable for widespread use.

The recommendations for the design of wide flange sections subject to flange curling and distortional or local buckling, presented in Part 2, are based on relatively few results and additional data are required to support the findings. Future studies which examine the interaction of distortional and local buckling failure modes of wide flange sections would provide valuable insights regarding the significance of flange curling on interaction failure. Also, the theoretical nonlinear flange curling model presented in this study can be made

more sophisticated by i) including the effects of material nonlinearity, and ii) considering the shift in the neutral axis due to plastic hinge formation in highly stressed regions. Consideration should also be given to the initial geometric imperfections and how they influence the flange curling behaviour and the failure mode.

## REFERENCES


1. AISI.(1968). "Specification for the Design of Cold-formed Steel Structural Members."AISI,Washington, D.C.
2. Akhand, A. M., Badaruzzaman, W. H. W., and Sanjery, K. A. (2004). "Ultimate Strength of aContinuous Decking of Cold-drawn Low-ductility High Strength Steel." Proc., 17th
3. Specialty Conference on Cold-Formed Steel Structures, November 2004, Orlando,Florida.
4. AS/NZS:4600. (1996). "Cold-Formed Steel Structures."Australian Standard/New ZealandStandards 4600:1996, Standards Australia, Sydney, Australia.
5. AS/NZS:4673. (2001). "Cold-Formed Stainless Steel Structures."Australian Standard/NewZealand Standard 4673:2001, Standards Australia, Sydney, Australia.
6. Bernard, E. S., Bridge, R. Q., and Hancock, G. J. (1993a). "Intermediate Stiffeners in Cold-Formed Profiled Steel Decking Part 3- Condeck Rolled Panels." Research Report No.R674, Department of Civil Engineering, University of Sydney, Sydney.
7. Desmond, T. P., Pekoz, T., and Winter, G. (1981b). "Intermediate Stiffeners for Thin-WalledMembers." Journal of the Structural Division, 107(ST4), 627-648.
8. Euro-Inox.(2002). "Design Manual for Structural Stainless Steel." Second Edition, Euro InoxandThe Steel Construction Institute.
9. Walker, A. C. (1975). Design and Analysis of Cold-Formed Sections, International TextbookCompany Ltd., London.
10. Winter, G. (1940)."Stress Distribution in and Equivalent Width of Flanges of Wide, Thin-Walled Steel Beams."NACA Technical Note(784).
11. Winter, G. (1947)."Strength of Thin Steel Compression Flanges." Transactions, 112, 527-554.